

This is an Open Access document downloaded from ORCA, Cardiff University's institutional repository:<https://orca.cardiff.ac.uk/id/eprint/118812/>

This is the author's version of a work that was submitted to / accepted for publication.

Citation for final published version:

El Albani, Abderrazak, Mangano, M. Gabriela, Buatois, Luis A., Bengtson, Stefan, Riboulleau, Armelle, Bekker, Andrey, Konhauser, Kurt, Lyons, Timothy, Rollion-Bard, Claire, Bankole, Olabode, Baghekema, Stellina G. L., Meunier, Alain, Trentesaux, Alain, Mazurier, Arnaud, Aubineau, Jeremie, Laforest, Claude, Fontaine, Claude, Recourt, Philippe, Chi Fru, Ernest, Macchiarelli, Roberto, Reynaud, Jean Yves, Gauthier-Layaye, Francois and Canfield, Donald E. 2019. Organism motility in an oxygenated shallow-marine environment 2.1 billion years ago. *Proceedings of the National Academy of Sciences* 116 (9), pp. 3431-3436. 10.1073/pnas.1815721116

Publishers page: <https://doi.org/10.1073/pnas.1815721116>

Please note:

Changes made as a result of publishing processes such as copy-editing, formatting and page numbers may not be reflected in this version. For the definitive version of this publication, please refer to the published source. You are advised to consult the publisher's version if you wish to cite this paper.

This version is being made available in accordance with publisher policies. See <http://orca.cf.ac.uk/policies.html> for usage policies. Copyright and moral rights for publications made available in ORCA are retained by the copyright holders.



Organism motility in an oxygenated shallow-marine environment 2.1 billion years ago

Abderrazak El Albani¹, Maria Mangano², Luis Buatois², Stefan Bengtson³, Armelle Riboulleau⁴, Andrey Bekker⁵, Kurt Konhauser⁶, Timothy Lyons⁷, Claire Rollion-Bard⁸, Olabode Bankole¹, Stellina Lekele Baghekema¹, Alain Meunier⁹, Alain Trentesaux¹⁰, Arnaud Mazurier¹, Jeremie Aubineau¹, Claude Laforest¹, Claude Fontaine⁹, Philippe Recourt¹¹, Ernest Chi Fru¹², Roberto Macchiarelli¹³, Jean Yves Reynaud¹⁴, François Gauthier-Layaye¹⁵, Donald Canfield¹⁶

¹University of Poitiers, ²University of Saskatchewan, ³Swedish Museum of Natural History, ⁴Université Lille1, ⁵University of California, Riverside, ⁶Uni. Alberta, ⁷University of California Riverside, ⁸Institut de Physique du Globe de Paris, ⁹Université de Poitiers, ¹⁰Lille 1 University, ¹¹University of Lille Nord de France, ¹²Cardiff University, ¹³Université de Poitiers, ¹⁴University of Lille, ¹⁵University of Strasbourg, ¹⁶Institute of Biology and Nordic Center for Earth Evolution (NordCEE), University of Southern Denmark

Submitted to Proceedings of the National Academy of Sciences of the United States of America

Evidence for macroscopic life in the Paleoproterozoic Era comes from 1.8 billion-year-old (Ga) compression fossils [Han TM, Runnegar B (1992), *Science* 257(5067):232-235; Knoll et al. (2006), *Philos Trans R Soc London B* 361(1470):1023-1038], Stirling biota [Bengtson S et al. (2007), *Paleobiology* 33(3):351-381], and large colonial organisms exhibiting signs of coordinated growth from the 2.1 Ga Francevillian Series, Gabon. Here we report on pyritized string-shaped structures from the Francevillian Basin. Combined microscopic, microtomographic, geochemical, and sedimentologic analyses provide evidence for biogenicity, and syngenetic and suggest that the structures underwent fossilization during early diagenesis close to the sediment-water interface. The string-shaped structures are up to 6 mm across and extend up to 170 mm through the strata. Morphological and 3D tomographic reconstructions suggest that the producer may have been a multicellular or syncytial organism able to migrate laterally and vertically to reach food resources. A possible modern analogue is the aggregation of amoeboid cells into a migratory slug phase in cellular slime molds at times of starvation. This unique ecologic window established in a oxygenated, shallow-marine environment represents an exceptional record of the biosphere following the crucial changes that occurred in the atmosphere and ocean in the aftermath of the Great Oxidation Event (GOE).

Motility | Paleoproterozoic Era | Oxygenation | Francevillian

The exquisitely preserved sediments of the Francevillian Series B (FB) Formation from southeastern Gabon were deposited in an oxygenated (1, 2) offshore to offshore transition environment at 2100 ± 30 million years ago (Ma) (3, 4). The deposits pass upwards into shallow-water, stromatolitic dolostones and dolomitic cherts of the Francevillian C (FC) Formation (*SI Appendix*, Figs. S1 and S2), recording a regression (1, 2). The specimens for this study were collected from black, silty shale intercalated with siltstone to very fine-grained sandstone in the FB₂ Member of the FB Formation (*SI Appendix*, Figs. S1 and S2).

The black, silty shales preserve millimetre-sized, diverse string-shaped structures (Figs. 1, 2), most of which are pyritized. These structures occur throughout the member; however, they are most abundant in the basal-most metre on the bedding plane (Fig. 1 and *SI Appendix*, Fig. S1C). Microbially induced sedimentary structures (MISS) prevail in the interbedded sandstone and silty sandstone layers (*SI Appendix*, *SI Text* 1, Fig. S3) and are commonly present in the vicinity of the string structures (Fig. 1E, F, I, J).

More than 80 specimens from several fossiliferous horizons were studied using X-ray micro-computed tomography (micro-CT) (Fig. 2; *SI Appendix*, Figs. S4-7 and Videos S1-4). The analysis reveals the presence of string-shaped structures within the strata (Fig. 2; *SI Appendix*, Figs. S4-7 and Videos S1-5). Some of these structures occur close to pyritized laminae lenses extending over

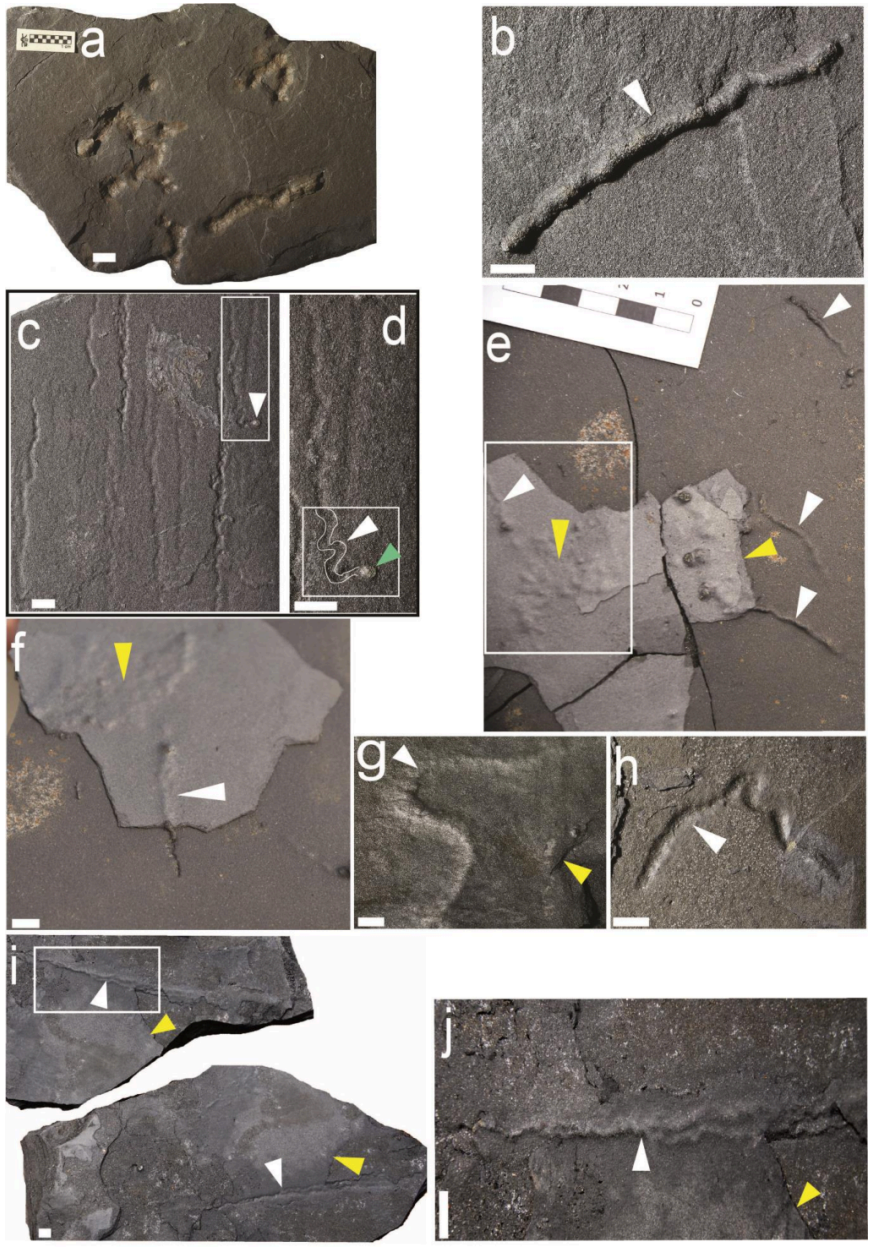
several centimetres (Figs. 2C-F and *SI Appendix*, Videos S1-3), suggesting an association with organic-rich mats where microbial sulphate-reduction was enhanced (Figs. 2C-F; *SI Appendix*, Figs. S3, S5-7). In one case, a sheet-like structure with distinct boundary forms an apparent continuity with an equally distinct string (Fig. 3A, B). Strings are mostly parallel to the bedding plane, and when observed in vertical cross-sections (Figs. 2C-F; *SI Appendix*, Fig. S6 and Videos S1, S2) display an elliptic to rounded section, flattened parallel to the bedding (Figs. 4C, E; *SI Appendix*, Fig. S6). They appear to have only a minor impact on the original sedimentary fabric with the laminae generally bending around these structures consistent with their early formation (Fig. 2H; *SI Appendix*, Figs. S6-7 and Videos S1-2). Specifically, the features indicate compaction of soft, fine-grained sediment around a relatively rigid object and show that the strings were in place and mineralized when the sediments were still compacting (Fig. 2H). Detrital phyllosilicate particles are parallel to bedding and aligned along the perimeter of the strings (Fig. 4). This relationship confirms pre-compactional formation of pyrite within the string structures resulting in local rearrangement of sediment grains during compaction. Combined SEM-BSE (scanning electron microscopy-back-scattered electron imaging) and EDX (energy-dispersive X-ray spectrometry) analyses also indicate

Significance

The 2.1 billion-year-old sedimentary strata contain exquisitely preserved fossils that provide an ecologic snapshot of the biota inhabiting a oxygenated, shallow-marine environment. Most striking are the pyritized string-shaped structures, which suggest that the producer have been a multicellular or syncytial organism able to migrate laterally and vertically to reach for food resources. A modern analogue is the aggregation of amoeboid cells into a migratory slug phase in modern cellular slime molds during time of food starvation. While it remains uncertain whether the amoeboid-like organisms represent a failed experiment or a prelude to subsequent evolutionary innovations, they add to the growing record of comparatively complex life forms that existed more than a billion years before animals emerged in the late Neoproterozoic.

Reserved for Publication Footnotes

137
138
139
140
141
142
143
144
145
146
147
148
149
150
151
152
153
154
155
156
157
158
159
160
161
162
163
164
165
166
167
168
169
170
171
172
173
174
175
176
177
178
179
180
181
182
183
184
185
186
187
188
189
190
191
192
193
194
195
196
197
198
199
200
201
202
203
204



PDF

Fig. 1. Reflected-light photographs of pyritized string-shaped specimens from the Francevillian Series, Gabon. White and yellow arrows point to string-shaped specimens and microbial mats, respectively. (A) Slab displaying several straight specimens with straight to convoluted strings. (B-I) Sinuous strings. (C) Straight or slightly contorted strings; frame denotes specimen figured in D. (D). Enlarged part of C, contour of trace marked in white within frame. Note the termination of the trace showing a small pyrite globule (green arrow). (E) Slab displaying several sub-parallel specimens in the vicinity of bacterial mats. Note that the relief increase at the surface of the sediment from right to left for each specimen; frame denotes specimen figured in F. (F) enlarged part of E, white arrow shows the detail of the trajectory of specimen under the fine clay laminae toward the bacterial mats (yellow arrow). (I, J) Part and counterpart of twinned contorted strings, parting from each other at upper white arrow; box denotes specimen figured in K. (K) Enlarged part of J; note the contorted strings and braided aspect. Scale bars are 1 cm.

205
206
207
208
209
210
211
212
213
214
215
216
217
218
219
220
221
222
223
224
225
226
227
228
229
230
231
232
233
234
235
236
237
238
239
240
241
242
243
244
245
246
247
248
249
250
251
252
253
254
255
256
257
258
259
260
261
262
263
264
265
266
267
268
269
270
271
272

contrasting textures and mineralogical compositions within and outside the strings (Figs. 4E, F). Very few detrital minerals (e.g., quartz) are scattered within the pyrite strings, while authigenic illite and chlorite grains show signs of free growth within the pore spaces (Figs. 4E, F, G).

The strings have a straight to sinuous shape (Figs. 1, 2; *SI Appendix*, Figs. S4, S-8) and a maximum length of 170 mm. The simplest specimens are horizontal, unbranched, with straight (Figs. 1A-B and 2A-B; *SI Appendix*, Fig. S6 and Video S3) to sinuous shapes (Figs. 1C-J; *SI Appendix*, Figs. S6-8 and Videos S1-2). They are 1-6 mm wide, with a relatively constant diameter along the structures (Figs. 2C-H; *SI Appendix*, Video S3). A rounded termination is typically observed at the end of the structures (Figs. 1 and 2A), but one specimen ends with a spheroidal pyrite concretion showing a similar size to the string structure (Figs. 1C, D; 2A, inset). Specimens may develop a short, low-wavelength sinuosity and angular bends (Figs. 1D, C, I, J). In some cases, there are two or more parallel strings (Figs. 1C,

D, I, J) that may intertwine and display a contorted helicoid shape, in places involving several strings in a braided pattern (Figs. 1I, J, 2G, H; *SI Appendix*, Fig. S4 and Video S4). X-ray micro-CT and petrographic microscopy reveal that these string-shaped structures also intersect the stratification (Figs. 2E; *SI Appendix*, Figs. S7-8 and Videos S-2). Strings might traverse silty-shale laminae and continue along at other levels, with angles of penetration ranging from 12 to 85° (Figs. 2D-F, 4E; *SI Appendix*, Figs. S5C, S8 and Videos S1-2).

The pyritized string structures are present in sediment deposited under oxygenated bottom-water conditions (1, 5). This is consistent with the observation that selective pyritization preferably occurs in oxic, organic-lean sediments, because localized organic enrichments favour the needed chemical gradients. The pyrite structures display highly negative $\delta^{34}\text{S}$ values (-31‰ to -21‰; *SI Appendix*, Figs. S9-10 and Table S1), which are in the range of the lightest values for sedimentary pyrite deposited

273
274
275
276
277
278
279
280
281
282
283
284
285
286
287
288
289
290
291
292
293
294
295
296
297
298
299
300
301
302
303
304
305
306
307
308
309
310
311
312
313
314
315
316
317
318
319
320
321
322
323
324
325
326
327
328
329
330
331
332
333
334
335
336
337
338
339
340

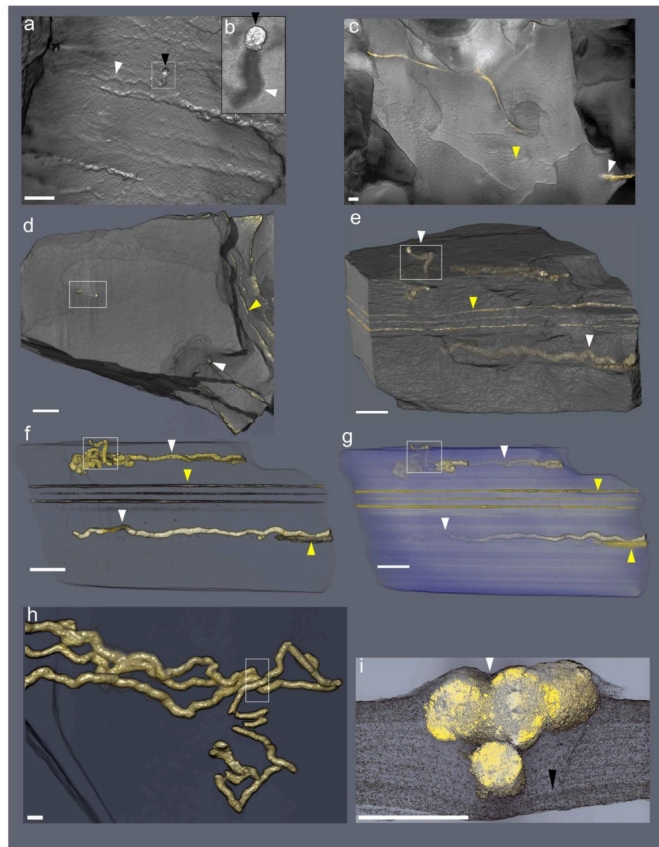


Fig. 2. Micro-CT-based reconstructions of string-shaped structures from the Francevillian Series, Gabon. White and yellow arrows point to string-shaped specimens and microbial mats, respectively. (A) Volume rendering showing the external surface of straight structures. Inset shows enlargement of string ending with a pyrite crystal. Same specimen as in Figures 1D and E. (B) External surface volume rendering showing weakly sinuous string. (C) External surface volume rendering, frame denotes the position of sub-vertical tubes. (D) External volume transparencies of the same specimen as in C, lateral view showing the string-shaped specimens inside the host rock. Frame denotes the position of sub-vertical tubes. (E, F) External volume transparencies of the same sample as in C and D at different heights in the sample. (G) Twinned contorted strings; box denotes portion (cross-section) figured in H. (H) Virtual cross-section of contorted strings, black arrow points to the pre-compactional deformation of silty-shale laminae. Scale bars are 1 cm.

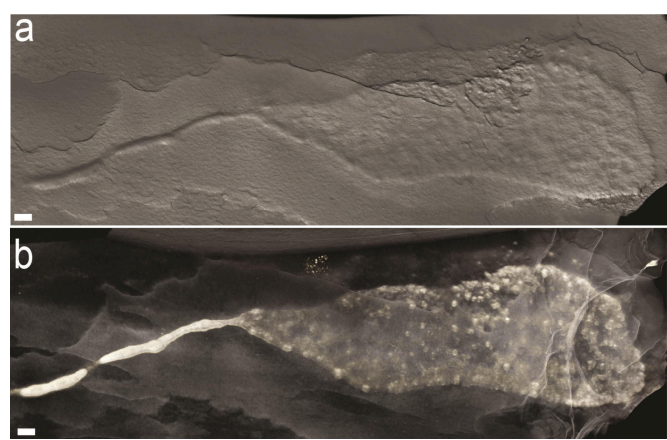


Fig. 3. (A, B) Volume rendering showing continuity between sheet and string morphologies in a single specimen. Scale bars are 1 cm

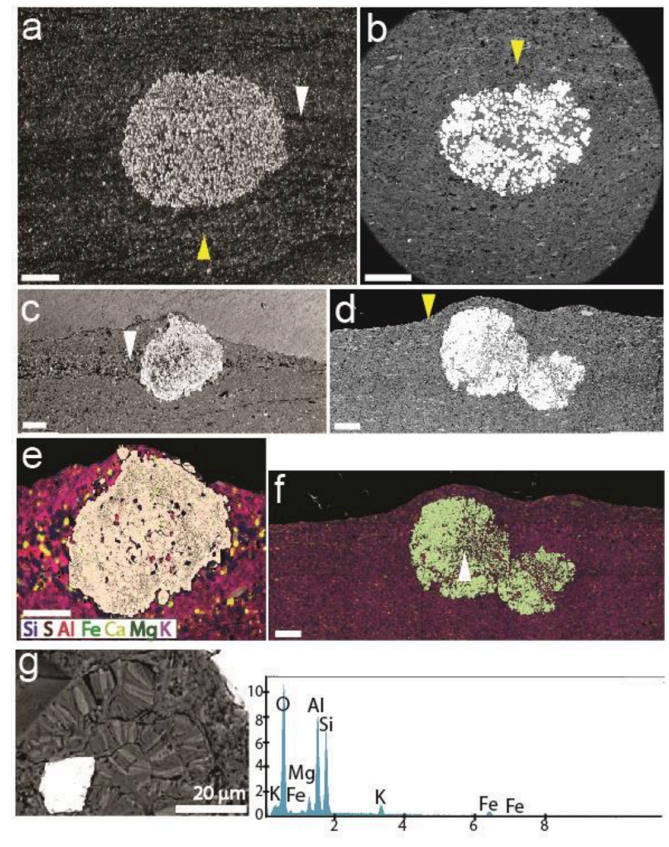


Fig. 4. Petrography with scanning electron microscopy (SEM) and energy dispersive analysis system (EDX) of pyritized string-shaped structures from the Francevillian Series, Gabon. (A, C). Sediment laminae, white arrow, intersected by pyritic strings. Laminae bending around the pyrite string confirm pre-compactional formation, yellow arrow. (B, D) Bending of sediment layers, yellow arrows, around pyritic strings. (E, F) Element mapping of sections in C and D, showing mineralogical composition of the strings and embedding sediment. White arrow indicates the area of elemental point analyses (G). Scale bars are 1 cm. (G) Elemental points analysis indicate the presence of K, Mg and Fe which confirm respectively the presence of illite and chlorite. The picture (left side) shows authigenic illite and chlorite grains and free growth of these minerals within the pore spaces.

before the late Neoproterozoic Era (6, 7). Considering a $\delta^{34}\text{S}$ value of $\sim 15\%$ for seawater sulphate at 2.1 Ga (6, 8), the low $\delta^{34}\text{S}$ values of the string-shaped structures indicate early diagenetic pyrite formation from sulphide generated by sulphate-reducing microorganisms close to the sediment-water interface from a relatively large seawater sulphate pool (12–14). Consistent with this observation, recent results suggest that concentration of sulphate in seawater may have been unusually high at this time, much higher than levels present immediately before and after this period of the Paleoproterozoic Era (12, 13).

The morphological patterns of the string-shaped structures and their relationship with the host sediment are very similar to those of burrows preserved through selective pyritization of mucus (14, 15), suggesting that the Francevillian structures may also be the result of early pyritization of a mucus strand. Nonetheless, it is critical to explore first the possibility of an abiogenic origin for the morphologies by making comparison with abiogenic structures. Detailed comparison with syneresis cracks and pyrite precipitated from migrating fluids (see *SI Appendix, SI Text 2, Fig. S11 and Table S2*) indicates that the mineralogy, 3D morphology, texture, and sulphur isotope composition of the Francevillian string-shaped structures are markedly different from these abiogenic structures.

341
342
343
344
345
346
347
348
349
350
351
352
353
354
355
356
357
358
359
360
361
362
363
364
365
366
367
368
369
370
371
372
373
374
375
376
377
378
379
380
381
382
383
384
385
386
387
388
389
390
391
392
393
394
395
396
397
398
399
400
401
402
403
404
405
406
407
408

409 The pyritic strings described herein may sometimes look
410 similar to other elongated body fossils in the Gabon biota, partic-
411 ularly where secondary pyritization has affected the morphology.
412 Lobate body fossils previously reported from these beds in places
413 may have a narrow, tail-like appendix that in well-preserved spec-
414 imens shows a flat cross-sectional profile and the same pattern
415 of radiating fabric and transverse folding characteristic of the
416 main body (14, 15). In heavily pyritized specimens, these primary
417 features are obscured, resulting in featureless rods. These fossils
418 resemble the specimen in Figure 3 (see, e.g., figures 4C, D, 5,
419 and 6E, F in (5)), but are usually coarser and display the typical
420 fabric of the lobate fossils. Another fossil that may have similarity
421 to string-shaped structures is a hitherto undescribed body fossil
422 forming a network of interconnected rings, where the walls are
423 expressed as thin pyritic strands along the bedding plane (*SI*
424 *Appendix, SI Text 3* and Fig. S12). Short fragments of this fossil
425 missing the branching points may be mistaken for the string
426 structures on the bedding plane.

427 Experimental work (16) has shown that an oscillatory flow
428 may interact with centimetric microbial aggregates, resulting in
429 the formation on the sediment surface of elongate structures that
430 may vaguely resemble the Francevillian string-shaped structures.
431 However, the latter shows clear evidence of emplacement within
432 the sediment. In addition, formation of the Francevillian Series B
433 below the fair-weather wave base is inconsistent with continuous
434 wave agitation.

435 A pyritized string of organic matter may represent the body
436 of a filamentous organism or it may be the remnants of an
437 organic tube or a mucus strand constructed by a motile organism.
438 Among filamentous organisms, the closest living analogues to the
439 Francevillian straight-to-sinuuous structures are sulphur-oxidizing
440 bacteria, such as *Thioploca* and *Beggiatoa*. These occur as hor-
441 izontally to vertically oriented sheathed filaments or filament
442 bundles in sediment, thriving at the interface between a weakly
443 oxic sediment–water interface and underlying reducing sediments
444 (17, 18). Individual filaments generally have a diameter of a
445 few to tens of micrometres, although giant *Beggiatoa* filaments
446 may reach nearly 200 µm in diameter (18). Sheathed *Thioploca*
447 filaments bundles with up to 500 µm diameter have been recorded
448 (17). The mucus sheaths of these sulphur-oxidizing bacteria allow
449 filaments to migrate in the sediment between the surficial, and the
450 deeper portions (17). Importantly, these microbial structures are
451 much smaller than ours. Phanerozoic pyritized organic trails and
452 burrows of dimensions comparable to those of the Francevillian
453 structures are commonly ascribed to animals (15, 19), but net-
454 works of pyritic filaments less than 1 mm in diameter have been
455 interpreted as bacterial or fungal in origin (15).

456 Other than length differences, the distinction between pyri-
457 tized tubes and trace fossils is subtle, but the latter can also be
458 recognized by being massive and locally branching and through
459 their incorporation of extraneous material (19). The Francevillian
460 structures reported herein conform to this pattern and thereby
461 resemble traces left by motile organisms, rather than individ-
462 ual filaments of bacteria or sheaths/tubes. They are somewhat
463 reminiscent of simple straight forms resembling grazing trails
464 in Ediacaran sedimentary successions, commonly in association
465 with microbial mats (23–25). However, unlike these Ediacaran
466 trails, the Francevillian structures have rounded terminations
467 and occasional bulbous elements. Moreover, characteristic levees
468 formed by sediment pushing on both sides, crucial in ascertaining
469 the locomotory origin of some of the Ediacaran trace fossils, are
470 absent in the Francevillian structures. In addition, a metazoan
471 origin would not be supported by evidence from molecular clocks
472 and the fossil record, which suggest a much younger origin for
473 animals at ~650 my ago (23, 24).

474 Although the Francevillian specimens tend to be oriented
475 parallel to bedding, they are occasionally oblique to subvertical
476

477 in orientation, crossing up to 1.5 cm of sediment and locally
478 disturbing primary laminations. These relationships can be taken
479 as evidence for movement within the sediment, consistent with
480 the absence of levees, which form in association with trails at
481 the sediment–water interface, or even as tool marks produced by
482 microbial aggregates moving under oscillating flow regimes (25).
483 Given the inconsistencies with traces produced by animals or with
484 sheaths enveloping motile bacteria, an alternative interpretation
485 should be sought to explain their generation. Production by a
486 microbial organism seems highly unlikely due to the lack of
487 empirical evidence that such organism can produce megascopic
488 infaunal trace fossils. There is no easy explanation, owing to
489 morphologic simplicity of the structures and their great age,
490 but a possible analogue for the formation of these structures
491 involves cellular slime molds, a group within Mycetozoa referred
492 to as Dictyosteliida (29–31). These organisms, as illustrated by
493 *Dictyostelium discoideum* and *D. polycephalum*, spend most of
494 their life cycle as individual amoebae feeding on bacteria, but
495 when food becomes scarce, single cells may aggregate to form a
496 multicellular organism, referred to as "a slug", that subsequently
497 moves on and within the sediment in search of a place for sporula-
498 tion (31–34). During their aggregation stage, slime molds display
499 behaviour that is remarkably similar to that of simple animals
500 (31).

501 The overall morphology of the Francevillian structures sug-
502 gests an organism that was able to aggregate and migrate in a
503 similar fashion to that of cellular slime molds, leaving a mucus
504 trail behind. The occasional continuity between sheet and string
505 morphology (Fig. 3) is particularly suggestive of this kind of
506 behaviour. The slug phase of cellular slime molds can develop
507 differences in speed, with faster anterior relative to the posterior
508 portion of the aggregate, resulting in a narrow isthmus between
509 the anterior and posterior parts (28). The bulbous elements and
510 the globular morphology of some of the string structures may
511 have resulted from this movement pattern. Since metazoan trace
512 fossils essentially reflect the maximum width of the producer,
513 burrows tend to display constant diameter, but this is not neces-
514 sarily the case with locomotive structures produced by mobile
515 cell aggregates. The broken and crenulated appearance of some
516 strings (Figs. 2E–G) is consistent with slugs crossing over each
517 other, resulting in the grafting of tips onto the slug as has been
518 observed in cellular slime molds during aggregation (28). In some
519 cases, the tips of two slugs going in the same direction may fuse
520 producing a larger one. The tip of the aggregate may also split
521 into two in a process known as twinning (28). In addition, parallel
522 orientation of some structures may reflect parallel movement
523 of the aggregates, as has been commonly observed in modern
524 dictyostelid slugs that move along environmental gradients (32).
525 The morphologic variability and intergradation of forms observed
526 in the Francevillian structures (Fig. 1), in particular the transfig-
527 uration between sheets and strings (Fig. 3), as well as grafting
528 and twinning of strings (Figs. 1I, J, 2G, H; *SI Appendix*, Fig.
529 S4), suggest locomotion of cell aggregates rather than organisms
530 having a distinct body shape and the presence of an interactive
531 sensorial system that reflects deliberate behaviour.

532 Structures consisting of pairs of ridges preserved in positive
533 hyporelief in *Myxomitodes* of the 2.0–1.8 Ga Stirling biota have
534 been interpreted as mucus-supported trails of syncytial or multi-
535 cellular organisms comparable to dictyostelid slime molds (33).
536 The Francevillian structures, which are up to ~300 million years
537 older than the Stirling biota, contrast with *Myxomitodes* in their
538 shape and dimensions. Again, the Francevillian features were
539 formed within the sediment as indicated by their oblique and
540 subvertical orientations to sediment lamination and in association
541 with matgrounds (Figs. 2B–F), whereas *Myxomitodes* is exclusively
542 parallel to the bedding and interpreted as having been formed at
543 the sediment–water interface (33).
544

Regardless of the difficulties in distinguishing between body and trace fossils, the interpretation of the Francevillian structures as those produced by organisms comparable in behaviour to cellular slime molds is consistent with their morphologic variability and mode of occurrence. The stimulus to become multicellular for dictyostelids is the lack of food (31–34)

Thus, the aggregative stage of slime molds could take place when all available organic material has been consumed. The Francevillian structures tend to occur next to matgrounds (Figs. 2C–F), which are abundant and regularly spaced vertically. A plausible ecosystem structure includes a community of single (non-aggregated), amoeba-like organisms thriving on buried microbial mats, but aggregating during times of starvation in order to move within the sediment to reach another mat at a different level. This mode of existence is consistent with movement guided by chemotaxis, which has been documented in modern dictyostelid slugs (27, 28). Slime molds have been observed to move vertically through sediment layers that are up to 7 cm thick (31, 32), showing the capability to penetrate the substrate in a way analogous to a muscular organism. This pattern is consistent with the localized vertical displacement revealed by the Francevillian structures. In addition, very shallow matgrounds could have enhanced oxygen concentrations creating oases rich in oxygen within the sediment at depths shallow enough to still receive light (34) (*SI Appendix, SI Text 1*). Modern studies have shown that during the day, concentrations of oxygen within biomats can be up to four times higher than in the oxygen-stressed overlying water column, highlighting the role of biomats as both oxygen and food resource during the Precambrian (34).

However, there are two significant differences between the Francevillian structures and those formed by modern slime molds. First, slime molds live in soils, not in marine sediment (28). In open-marine environments, the chemical gradients that are necessary for the amoeboid cells to aggregate are not observed at the surface of sediments, but frequently develop within the sediment as a result of microbial activity and sediment permeability. This argument is strong in rejecting a slime-mold interpretation in the case of the surface trace *Myxomitodes* (33). Unlike *Myxomitodes*, the Francevillian structures were formed within a fine-grained and overall undisturbed sediment, where the development of chemical gradients was favoured. Second, the width of modern slime-mold slugs is up to 0.2 mm, significantly smaller than that of the structures documented here. Importantly, we are not suggesting that the Francevillian structures were produced by slime molds, although the size and complexity of the fossils suggest that the organism may have been a eukaryote. We rather advocate an analogous situation wherein amoeba-like organisms with the capability to aggregate in a similar fashion could have been responsible for producing these complex structures. The restriction of modern dictyostelids to soils does not rule out the possibility that amoeba-like organisms may have been able to evolve the trait of aggregation in marine environments below the sediment-water interface, particularly in microbially bound sediments.

The timing of origin of eukaryotes and its potential link to the GOE has been the focus of intense debate (35–37). Integration of genomic and fossil evidence suggests that eukaryotes emerged approximately 1.84 Ga ago, therefore postdating the GOE (Betts et al., 2018) and the Francevillian structures, which correspond in age to the end of the Lomagundi Event (~2.22 to 2.06 Ga). This event represents, the largest global positive C isotope excursion in Earth's history, which is recorded in the FB and FC formations of the Francevillian Series (2). This excursion is thought to reflect a time of relatively high oxygen content in the atmosphere and ocean relative to the time intervals immediately before and after (38). Regardless of the approximately 300 million years discrepancy between the Francevillian and the proposed

timing for origin of eukaryotes, it is reasonable to assume that such an increase in oxygenation may have promoted evolutionary innovations, such as those recorded by the Gabonese biota and associated ecosystems (El Albani et al., 2010, 2014; Aubineau et al., 2018).

The Lomagundi Event may have ended up with a dramatic deoxygenation after which seawater O₂ levels remained near or below the lower limit necessary for complex life to survive until the late Neoproterozoic (39). In addition to this broad temporal relationship with an oxygen increase, the FB and FC formations were deposited in nearshore to offshore environments that allowed widespread development of microbial mats (*SI Appendix, Fig. S3*). These shallow-water, oxygen and food-rich conditions within the photic zone were instrumental for the establishment of an ecosystem able to harbour more advanced forms of life, including organisms that could migrate. The fossiliferous Francevillian strata were ultimately preserved in essentially undeformed and non-metamorphosed strata (40). These special conditions underscore the uniqueness of the Francevillian biota, although it cannot be entirely excluded that our occurrence is related more to favourable taphonomic conditions than to environmental or evolutionary drivers/patterns. While it remains uncertain whether the Francevillian string-shaped structures represent a failed experiment or a prelude to subsequent evolutionary innovations, they add to the growing record of comparatively more complex life forms that colonized shallow-marine environments more than a billion years before animals emerged in the late Neoproterozoic.

Methods

Textural relationships between the pyritized string-shaped structures and the silty shale matrix embedding the structures were assessed on polished slab sections with a ZEISS Discovery V8 stereoscope combined with AxioCam ERc 5s microscope camera. SEM was carried out on a JEOL 5600 LV equipped with an Oxford EDX for mineralogical analyses.

The micro-CT analysis of the samples was run on a RX-solutions EasyTom XL Duo equipment, which has one micro- and one nanofocus (LaB6 filament) Hamamatsu X-ray sources coupled to a Varian PaxScan 2520DX flat panel. Reconstructions were done with the XAct software (RX-solutions) with a classical filtered back projection algorithm and reduction of beam hardening artefact. *Virtual sections, 3D rendering, and videos were performed with Avizo Fire v.9.2 (FEI)*.

Values of $\delta^{34}\text{S}$ were measured with Secondary Ion Mass Spectrometry (SIMS) using a Cameca IMS1270 and 1280 at CRPG facility (Nancy, France). The sulphur isotope compositions were measured using a 20- μm Cs⁺ primary beam of ~2–5 nA. Sulphur isotopes were measured in a multi-collection mode using two off-axis Faraday cups (L2 and H1). The gains of the Faraday cups were intercalibrated at the beginning of the analytical session and their offsets were determined before each analysis during the pre-sputtering (300 s). Typical ion intensities of 3×10^9 counts per second (cps) were obtained on ³²S, so that an internal error better than ± 0.1 ‰ can be reached. Instrumental mass fractionation and external reproducibility were determined by multiple measurements of the in-house reference material Pyr3B ($\delta^{34}\text{S} = +1.41$ ‰). The external reproducibility ranges between 0.05 and 0.40 ‰ (1 sigma) depending on the analytical session.

Acknowledgements

We appreciate assistance from the Gabonese government, Centre National Pour la Recherche Scientifique & Technique du Gabon (CENAREST), General Direction of Mines and Geology of Gabon, Sylvia Bongo Ondimba Foundation, Agence Nationale des Parcs Nationaux du Gabon, University of Masuku, COMILOG and SOCOBA Companies, French Embassy at Libreville, Institut Français du Gabon, Le Centre National de la Recherche Scientifique (CNRS), and La Région Nouvelle Aquitaine for their supports. The authors acknowledge the support from RX-Solutions (Industrial X-Ray Tomography company), the Trace Analysis for Chemical, Earth and Environmental Sciences (TrACEES) platform from the Melbourne Collaborative Infrastructure Research Program at the University of Melbourne and P' Institute UPR 3346 from Poitiers University. For information and scientific discussion, we thank, P-D Mougouiana, F.D. Idiata, L. White, J.C. Baloché, R. Oslisly, F. Weber, A. Chirazi, F. Pambo, Idalina Moubiya Mouélé and J.L. Albert. For assistance, we acknowledge C. Lebaillly, Ph. Jalladeau, D. Autain and S. Riffaut and the administrative staff of the University of Poitiers. **Author contributions** A.E.A. conceived the project. A.E.A., G.M., L.B., S.B. and DEC. designed research. A.E.A., A.T., C.L., O.B., S.G.L.B., J.A., and F.G.L. performed field research. A.E.A., F.G.L., and A.T. J.Y.R. performed sedimentological analyses. G.M., L.B., S.B., and A.E.A. performed ichnological analyses. A.Ma. and R.M. performed microtomographic analyses. C.R.B. performed isotope analyses. Ph.R.

681
682
683
684
685
686
687
688
689
690
691
692
693
694
695
696
697
698
699
700
701
702
703
704
705
706
707
708
709
710
711
712
713
714
715
716
717
718
719
720
721
722
723
724
725
726
727
728
729
730
731
732
733
734
735
736
737
738
739
740
741
742
743
744
745
746
747
748

performed SEM analyses. D.E.C., T.L., A.B., K.K., E.C., and A.Me. provided critical input to the manuscript. A.E.A., G.M., L.B., S.B., and A.R. wrote the main part of the manuscript with input from all co-authors. **Author**

1. El Albani A, et al. (2010) Large colonial organisms with coordinated growth in oxygenated environments 2.1Gyr ago. *Nature* 466(7302):100–104.
2. Canfield DE, et al. (2013) Oxygen dynamics in the aftermath of the Great Oxidation of Earth's atmosphere. *Proc Natl Acad Sci USA* 110(42):16736–16741.
3. Bros R, Stille P, Gauthier-Lafaye F, Weber F, Clauer N (1992) Sm-Nd isotopic dating of Proterozoic clay material: An example from the Francevillian sedimentary series, Gabon. *Earth Planet Sci Lett* 113(1–2):207–218.
4. Horie K, Hidaka H, Gauthier-Lafaye F (2005) U-Pb geochronology and geochemistry of zircon from the Franceville series at Bidououma, Gabon. *Geochim Cosmochim Acta* 69(10 supplement):A11.
5. El Albani A, et al. (2014) The 2.1 Ga Old Francevillian Biota: Biogenicity, Taphonomy and Biodiversity. *PLoS ONE* 9(6):e99438.
6. Canfield DE, Farquhar J (2009) Animal evolution, bioturbation, and the sulfate concentration of the oceans. *Proc Natl Acad Sci USA* 106(20):8123–8127.
7. Zhelezinskaia I, Kaufman AJ, Farquhar J, Cliff J (2014) Large sulfur isotope fractionations associated with Neoproterozoic microbial sulfate reduction. *Science* 346(6210):742–744.
8. Guo Q, et al. (2009) Reconstructing Earth's surface oxidation across the Archean-Proterozoic transition. *Geology* 37(5):399–402.
9. Canfield DE (2001) Isotope fractionation by natural populations of sulfate-reducing bacteria. *Geochim Cosmochim Acta* 65(7):1117–1124.
10. Habicht KS, Gade M, Thamdrup B, Berg P, Canfield DE (2002) Calibration of sulfate levels in the Archean ocean. *Science* 298(5602):2372–2374.
11. Johnston DT, Farquhar J, Canfield DE (2007) Sulfur isotope insights into microbial sulfate reduction: When microbes meet models. *Geochim Cosmochim Acta* 71(16):3929–3947.
12. Planavsky NJ, Bekker A, Hofmann A, Owens JD, Lyons TW (2012) Sulfur record of rising and falling marine oxygen and sulfate levels during the Lomagundi event. *Proc Natl Acad Sci USA* 109(45):18300–18305.
13. Scott C, et al. (2014) Pyrite multiple-sulfur isotope evidence for rapid expansion and contraction of the early Paleoproterozoic seawater sulfate reservoir. *Earth Planet Sci Lett* 389(0):95–104.
14. Schieber J (2002) The role of an organic slime matrix in the formation of pyritized burrow trails and pyrite concretions. *Palaios* 17(1):104–109.
15. Virtasalo JJ, Löwemark L, Papunen H, Kotilainen AT, Whitehouse MJ (2010) Pyritic and baritic burrows and microbial filaments in postglacial lacustrine clays in the northern Baltic Sea. *J Geol Soc* 167(6):1185–1198.
16. Mariotti G, Pruss SB, Ai X, Perron JT, Bosak T (2016) Microbial Origin of Early Animal Trace Fossils? CURRENT RIPPLES. MARIOTTI ET AL. *Journal of Sedimentary Research* 86(4):287–293.
17. Jørgensen BB, Gallardo VA (1999) *Thioploca* spp.: filamentous sulfur bacteria with nitrate vacuoles. *FEMS Microbiol Ecol* 28(4):301–313.
18. Larkin J, Henk MC, Aharon P (1994) *Beggiatoa* in microbial mats at hydrocarbon vents in the Gulf of Mexico and Warm Mineral Springs, Florida. *Geo-Mar Lett* 14(2):97–103.
19. Thomsen E, Vorren TO (1984) Pyritization of tubes and burrows from Late Pleistocene continental shelf sediments off North Norway. *Sedimentology* 31(4):481–492.
20. Seilacher A, Buatois LA, Mángano MG (2005) Trace fossils in the Ediacaran–Cambrian transition: Behavioral diversification, ecological turnover and environmental shift. *Palaeogeogr*

Information Correspondence and requests for materials should be addressed to A.E.A. (abder.albani@univ-poitiers.fr). Declaration of competing interests
The authors declare no competing financial interests.

- Palaeoclimatol Palaeoecol* 227(4):323–356.
21. Jensen S, Droser ML, Gehling JG (2006) A Critical Look at the Ediacaran Trace Fossil Record. *Neoproterozoic Geobiology and Paleobiology*, eds Xiao S, Kaufman AJ (Springer Netherlands, Dordrecht), pp 115–157.
22. Buatois LA, Mángano MG (2016) Ediacaran Ecosystems and the Dawn of Animals. *The Trace-Fossil Record of Major Evolutionary Events: Volume 1: Precambrian and Paleozoic*, eds Mángano MG, Buatois LA (Springer Netherlands, Dordrecht), pp 27–72.
23. Cunningham JA, Liu AG, Bengtson S, Donoghue PCJ (2017) The origin of animals: Can molecular clocks and the fossil record be reconciled? *BioEssays* 39(1):1–12.
24. Love GD, et al. (2009) Fossil steroids record the appearance of Demospongiae during the Cryogenian period. *Nature* 457(7230):718–721.
25. Mariotti G, Pruss SB, Ai X, Perron JT, Bosak T (2016) Microbial shaping of sedimentary wrinkle structures. *J Sed Res* 86(4):287–293.
26. Hagiwara H (1991) A new species and some new records of dictyostelid cellular slime molds from Oman. *Bull Natn Sci Mus, Tokyo, Ser B* 17(3):109–121.
27. Kessin RH (2001) *Dictyostelium: evolution, cell biology, and the development of multicellularity* (Cambridge University Press).
28. Bonner JT (2009) *The social amoebae: the biology of cellular slime molds* (Princeton University Press).
29. Wallraff E, Wallraff HG (1997) Migration and bidirectional phototaxis in *Dictyostelium discoideum* slugs lacking the actin cross-linking 120 kDa gelation factor. *J Exp Biol* 200(24):3213–3220.
30. Sternfeld J, O'Mara R (2005) Aerial migration of the *Dictyostelium* slug. *Dev Groth Differ* 47(1):49–58.
31. Bonner JT (2006) Migration in *Dictyostelium polycephalum*. *Mycologia* 98(2):260–264.
32. Bonner JT, Lamont DS (2005) Behavior of cellular slime molds in the soil. *Mycologia* 97(1):178–184.
33. Bengtson S, Rasmussen B, Krapež B (2007) The Paleoproterozoic megascopic Stirling biota. *Paleobiology* 33(3):351–381.
34. Gingras M, et al. (2011) Possible evolution of mobile animals in association with microbial mats. *Nature Geosci* 4(6):372–375.
35. Schirrmeister BE, Vos JM de, Antonelli A, Bagheri HC (2013) Evolution of multicellularity coincided with increased diversification of cyanobacteria and the Great Oxidation Event. *PNAS* 110(5):1791–1796.
36. Knoll AH, Nowak MA (2017) The timetable of evolution. *Science Advances* 3(5):e1603076.
37. Betts HC, et al. (2018) Integrated genomic and fossil evidence illuminates life's early evolution and eukaryote origin. *Nature Ecology & Evolution* 2(10):1556.
38. Lyons TW, Reinhard CT, Planavsky NJ (2014) The rise of oxygen in Earth's early ocean and atmosphere. *Nature* 506(7488):307–315.
39. Planavsky NJ, et al. (2014) Low Mid-Proterozoic atmospheric oxygen levels and the delayed rise of animals. *Science* 346(6209):635–638.
40. Gauthier-Lafaye F, Weber F (2003) Natural nuclear fission reactors: time constraints for occurrence, and their relation to uranium and manganese deposits and to the evolution of the atmosphere. *Precamb Res* 120(1–2):81–100.

749
750
751
752
753
754
755
756
757
758
759
760
761
762
763
764
765
766
767
768
769
770
771
772
773
774
775
776
777
778
779
780
781
782
783
784
785
786
787
788
789
790
791
792
793
794
795
796
797
798
799
800
801
802
803
804
805
806
807
808
809
810
811
812
813
814
815
816